Pramana – J. Phys. (2018) 90:36
https://doi.org/10.1007/s12043-018-1523-3

Effect of three-body transformed Hamiltonian ($\tilde{H}_3$) using full connected triple excitation coupled cluster operators on valence ionisation potentials of Cl_2 and F_2 computed via EIP-VUMRCCSDτ scheme

KALIPADA ADHIKARI

Department of Physics, M.B.B. College, Agartala 799 004, India
E-mail: adhikarikalipada@gmail.com

MS received 6 March 2017; revised 26 September 2017; accepted 3 October 2017;
published online 13 February 2018

Abstract. Valence universal multireference coupled cluster (VUMRCC) method via eigenvalue independent partitioning has been applied to estimate the effect of three-body transformed Hamiltonian ($\widetilde{H}_3$) on ionisation potentials through full connected triple excitations $S_3^{(1,0)}$. $\widetilde{H}_3$ is constructed using CCSDT1-A model of Bartlett *et al* for the ground-state calculation. Contribution of transformed Hamiltonian through full connected triples $\overline{\widetilde{H}_3 S_3^{(1,0)}}$ involves huge amount of computational operations that is time-consuming. Investigation on Cl_2 and F_2 molecules using cc-pVDZ and cc-pVTZ basis sets shows that the above effect varies from 0.001 eV to around 0.5 eV, suggesting that inclusion of $\overline{\widetilde{H}_3 S_3^{(1,0)}}$ is essential for highly accurate calculations.

Keywords. Triple excitation; transformed Hamiltonian; ionisation potential.

PACS Nos **31.15.A–; 31.15.bw; 32.10.Hq; 33.15.Ry**

1. Introduction

Efficient incorporation of triple excitations [1] to evaluate electron correlations highly accurately in ground state and in ionised/excited states has now emerged as a field of much interest in quantum chemistry. Calculations using ADC(3)/ADC(4) method [2,3], state-specific multireference perturbation theory using Møller–Plesset multipartitioning of the Hamiltonian (IVO-SSMRPT) [4,5], MRCI method [6], SAC-CI (general-R) method [7–9], EOM-CC method [10–12], full EOMCCSDt method [13], state-specific multireference coupled cluster (SS-MRCC) method [14] etc. are some of the frontier theories in this respect. In many cases, electronic difference energies such as ionisation potentials (IP) are obtained within (or near to) 0.1 eV of experimental results.

The single reference theory (SRCC) truncated at the singles and doubles (SD) excited cluster level is not adequate for the state with multireference (MR) character. The coupled-cluster method is an attractive method in the field of electronic structure calculations. Theories designed explicitly to treat multireference (MR) systems have been under development since the early stage of coupled cluster theory. Valence universal (Fock space) multireference coupled cluster (VUMRCC) theory [15–21] is a very effective MR method for computing difference energies, such as IPs, double ionisation energies (DIP), excitation energies (EE) and electron affinity (EA). In VUMRCC theories, one universal wave operator is used for all sectors of Fock space. It works relative to a 'common vacuum' $|\Phi_{\mathrm{HF}}\rangle$, and the open-shell systems [22] are reached by changing the number of electrons from the reference state. Though originally developed as an effective Hamiltonian (H_{eff})-based theory [16], it now has alternative forms. The effective Hamiltonian method which involves nonlinear CC equations is prone to severe numerical divergence problems borne out of the well-known intruder states as one goes to determine the inner valence main IPs and the satellite IPs. The theory of incomplete model space [17] is one way to tackle the divergence problem to some extent. But this may not be adequate, considering the grave situation.

Using eigenvalue-independent partitioning (EIP) technique, Mukherjee and co-workers [23,24] have developed a novel alternative form of the effective Hamiltonian-based VUMRCC theory (coined as EIP-MRCC) which seems more like a CI-structure, despite it normally being non-Hermitian and also having 'hidden nonlinearity' in CC variables. The nonlinear VUMRCC equations and the equation for H_{eff} for any (m-hole, n-particle) model space (complete model space or incomplete model space) are converted into the respective set of non-Hermitian eigenvalue equations using eigenvalue independent partitioning technique (EIP) technique [23,25]. Starting with a suitable guess eigenvector, the desired solution of each low-lying root of spectroscopic interest is arrived at iteratively by using suitable root-search and root-homing procedures employed in the eigenvalue problems (see ref. [23]). The norm of the eigenvector of each root is preserved to unity in every iteration, and hence the method is less prone to divergence compared to even the VUMRCC theory for incomplete model space. Thus, the inner valence IPs along with most of the satellite IPs which cannot be obtained by solving the nonlinear CC equations can be calculated by applying the EIP-MRCC method. It is noteworthy that the EIP-MRCC equations for IP (1-hole, 0-particle problem) and for EA (0-hole, 1-particle problem) are identical with the respective SRCC-LRT equations [26].

Mukherjee and co-workers have done some initial pilot calculations at EIP-MRCCD level [23], where D represents doubles $S_2^{(0,0)} = T_2$ in the ground-state calculation (figure 1c), and doubles $S_2^{(1,0)}$ means ionisation with simultaneous single excitation (figure 1d). It is to be mentioned here that the IPs come out as direct difference energies, and they are size-intensive [24,27]. Using subsystem embedding condition (SEC) [19], DIPs related to Auger electron processes of HF molecule have been calculated by employing $S_2^{(1,0)}$ only. In the same way, EEs of N_2 have been calculated using $S_2^{(1,0)}$ and $S_2^{(0,1)}$, where the doubles $S_2^{(0,1)}$ represent electron attachment with simultaneous single excitation. Chaudhuri *et al* [28] studied IPs of HF and H_2O by EIP-MRCC method using singles $S_1^{(1,0)}$ and doubles $S_2^{(1,0)}$ and included the effect of connected triples $S_3^{(1,0)}$ perturbatively correct up to third order. It is to be emphasised that in their work, the back coupling of $S_3^{(1,0)}$ to $S_1^{(1,0)}$ and $S_2^{(1,0)}$ was ignored. But, in the present work, the connected triples $S_3^{(1,0)}$ and the doubles $S_2^{(1,0)}$ are fully coupled through eqs (11)–(13), thus taking into account higher-order perturbative terms systematically, if not fully. As we have kept all holes 'active', no $S_1^{(1,0)}$ appeared in the present calculations. In the ground-state CC calculation too, the two works differ significantly. While in the former work, no connected triples $S_3^{(0,0)} (= T_3)$ was considered in the ground-state CC calculation which was done at full CCSD level only, in our work, along with full CCSD, effect of connected triples has also been taken into account through the approximation $S_3^{(0,0)} = T_3 = \{\overline{VT}_2/\Delta\varepsilon\}_3$ as per the CCSDT1-A model for ground-state CC calculation, and iterations were repeated till convergence was reached. It is pertinent to mention that the CCSDT1-A method is known to have an excellent intrinsic accuracy for a wide variety of applications in quantum chemistry. It is important to note that in our work, there is no approximation in $S_3^{(1,0)}$ in the case of ionisation. Mitra *et al* [29] studied DIPs related to Auger electrons of NH_3, HCl and PH_3 using multiple solutions of $S_2^{(1,0)}$ obtained from eigenvectors of IP calculation at EIP-MRCCSD level. At EIP-MRCCSDτ level, which considers connected triples $S_3^{(0,0)} (= T_3)$ by CCSDT1-A approach [30] for ground state, and fully connected triples $S_3^{(1,0)}$, i.e., ionisation with simultaneous double excitations (figure 1e) for ionised states, Chattopadhyay *et al* [31] calculated only the IPs of outer valence

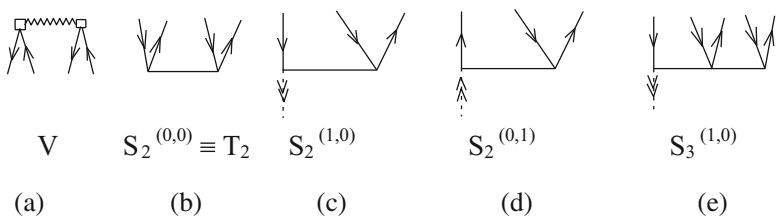

Figure 1. Downward arrow lines represent 'holes (h)' and upward arrow lines, 'particles (p)', and all double arrow lines are 'active'. (**a**) Normal ordered two-body part (V) of Hamiltonian H, (**b**) two-electron closed shell CC operators or doubles (D), (**c**) normal ordered two-electron operators for shake-up ionisation or doubles $S_2^{(1,0)}$, i.e., ionisation with simultaneous single excitation of electron, (**d**) normal ordered two-electron operators $S_2^{(0,1)}$ for electron attachment and (**e**) normal ordered three-electron operators for shake-up ionisation or triples $S_3^{(1,0)}$, i.e., ionisation with simultaneous double excitations of electrons. It is to be emphasised that the downward double arrow line underneath the $S^{(1,0)}$ vertex does not participate in the EIP-MRCCSDτ matrix construction.

regions of N_2 and CO using cc-pVXZ (X=D,T,Q) bases. Later on, Chattopadhyay *et al* [32] have calculated and analysed all valence main IPs along with outer valence shake-up and inner valence shake-up satellites of HF and HCl molecules using the same kind of basis sets. Comparison of the results generated via EIP-MRCCSDτ with experiments are highly encouraging and the results of all main IPs, except the first two IPs above 20 eV of HCl, are within (or very near to) 0.1 eV of experimental values. Adhikari *et al* [25] estimated the effect of three-body transformed Hamiltonian $\tilde{H}_3$ on the main and satellite ionisation potentials through fully connected triple excitations $S_3^{(1,0)}$ of HF, HCl, N_2 and CO with cc-pVDZ and cc-pVTZ basis sets using VUMRCC method via eigenvalue-independent portioning technique. Later on, Adhikari *et al* [33] have computed and analysed all valence main IPs along with outer valence shake-up satellites of C_2H_4 and C_2H_2 molecules using cc-pVXZ (X=D,T) bases and N_2 and CO molecules using cc-pVXZ (X=D,T,Q) bases. Results are in accord with the previously published experimental and other state-of-the-art theoretical observations.

2. Theory in brief

We choose the Hartree–Fock [34], SCF solution for the closed- shell N-electron ground state Φ_{HF} as the vacuum for labelling purposes, to define holes and particles with respect to Φ_{HF}. The multireference aspect is introduced by having hole and particle orbitals further subdivided into active and inactive groups. Different occupations of the active orbitals will define a multireference model space for our problem. In Fock-space notation, we designate by $\Psi^{(kh,lp)}$ a model space of *kh-lp* determinants, where in the present instance, k ranges from 0 to 1 and l equals 0.

To calculate the energies for the open-shell states like $(N-1)$ electron states or the excited N-electron states we substitute the form of the wave function in the Schrödinger equation for a manifold of states:

$$H|\Psi_i^{(k,l)}\rangle = E_i|\Psi_i^{(k,l)}\rangle \tag{1}$$

which leads to

$$H\Omega\left(\sum C_i\Phi_i^{(k,l)}\right) = E_i\Omega\left(\sum C_i\Phi_i^{(k,l)}\right), \tag{2}$$

where $\Phi_i^{(k,l)}$ are the determinants included in the model space $\Psi_i^{0(k,l)}$. We now define an effective Hamiltonian $H_{\mathrm{eff}}^{(k,l)}$ for the general k-active hole and l-active electron situation as

$$H_{\mathrm{eff}}^{(k,l)} = P^{(k,l)}\Omega^{-1}H\Omega P^{(k,l)}. \tag{3}$$

That is,

$$\left(H_{\mathrm{eff}}^{(k,l)}\right)_{ij} = \Phi_i^{(k,l)}\left|\Omega^{-1}H\Omega\right|\Phi_j^{(k,l)}, \tag{4}$$

where $P^{(k,l)}$ is the projection operator on to the model space defined by the linear combination of determinants having k-active holes and l-active particles, i.e., $\sum_i C_i\Phi_i^{(k,l)}$. With definition of $H_{\mathrm{eff}}^{(k,l)}$ as in eq. (3) or (4) we premultiply eq. (2) by Ω^{-1} and project the subsequent equation onto the model-space determinants. We readily see that it leads to an eigenvalue equation for $H_{\mathrm{eff}}^{(k,l)}$, where the eigenvalues of $H_{\mathrm{eff}}^{(k,l)}$ are the corresponding energies of k-active hole and l-active particle open-shell states. The Fock-space Bloch equation, an alternative form of Schrödinger equation, is expressed as

$$H\Omega P^{(k,l)} = \Omega H_{\mathrm{eff}}^{(k,l)}P^{(k,l)};\ 0 \le k \le m, 0 \le l \le n, \tag{5}$$

where Ω is the valence universal normal ordered wave operator and is expressed as

$$\begin{aligned}\Omega &= \left\{\exp\left(S^{(m,n)}\right)\right\}\\ &= \left\{\exp\left(\sum_{k=0}^{m}\sum_{l=0}^{n}S^{(k,l)}\right)\right\}.\end{aligned} \tag{6}$$

The curley bracket in eq. (6) denotes the normal ordering. $S^{(k,l)}$acts upon $P^{(k,l)}$space determinants to generate the virtual space Q and R space determinants.

Ω can also be expressed as

$$\Omega = \exp\left(S^{(0,0)}\right)\left\{\exp\left(S^{(m,n)}\right)\right\} = \Omega_c^{(0,0)}\Omega_v^{(m,n)}, \tag{7}$$

where $\Omega_c^{(0,0)}$ stands for the wave operator relating to the core electrons and gives the closed-shell cluster amplitude $\left(S^{(0,0)}\right)$. $\Omega_v^{(m,n)}$, in which $(k,l) \neq (0,0)$ stands for the wave operator for the valence electrons (three in the present work).

Mukherjee *et al* [23,24] first formulated EIP-VUMRCC theory for a general (incomplete or complete) model space on the basis of the work of Coope and Sabo [35]. In the EIP-VUMRCC framework, the ionisation potential calculation is called a [1,0] valence problem, and thus it includes the coupled cluster operators for (0,0) and (1,0) valence components. Consequently,

$$\begin{aligned}\Omega &= \left\{\exp\left(S^{(0,0)} + S^{(1,0)}\right)\right\}\\ &= \Omega_c^{(0,0)}\left\{\exp\left(S^{(1,0)}\right)\right\}\\ &= \exp(T_c)\{\exp(S)\},\end{aligned}$$

where T_c is a standard single reference cluster operator that acts on a single determinantal RHF and S represents the Fock-space cluster operator defined in a universal

manner for all sectors. With the help of the above definition of Ω, and projecting the Bloch equation (5) from the left on projector operators $P^{(k,l)}$, $Q^{(k,l)}$ and $R^{(k,l)}$ respectively, we can write the Bloch equation in the context of the VUMRCC scheme as

$$P^{(k,l)}\overline{\bar{H}\Omega_v}P^{(k,l)} = P^{(k,l)}\overline{\Omega_v H}_{\text{eff}}P^{(k,l)}, \tag{8}$$

$$Q^{(k,l)}\overline{\bar{H}\Omega_v}P^{(k,l)} = Q^{(k,l)}\overline{\Omega_v H}_{\text{eff}}P^{(k,l)}, \tag{9}$$

$$R^{(k,l)}\overline{\bar{H}\Omega_v}P^{(k,l)} = R^{(k,l)}\overline{\Omega_v H}_{\text{eff}}P^{(k,l)}, \tag{10}$$

where (k, l) stands for the Fock-space sector (denote the number of valence holes and particles respectively).

To compute ionisation potential, we can write the VUMRCC equations for effective Hamiltonian, eq. (8) and cluster operators, eq. (9), eq. (10), respectively, as follows:

$$P^{(1,0)}\tilde{H}P^{(1,0)} + P^{(1,0)}\left\{\overline{\tilde{H}S}^{(1,0)}\right\}P^{(1,0)} = \tilde{H}^{(1,0)}_{\text{eff}}, \tag{11}$$

$$Q^{(1,0)}\tilde{H}P^{(1,0)} + Q^{(1,0)}\left\{\overline{\tilde{H}S}^{(1,0)}\right\}P^{(1,0)} = Q^{(1,0)}\left\{\overline{S^{(1,0)}\tilde{H}_{\text{eff}}}\right\}P^{(1,0)}, \tag{12}$$

$$R^{(1,0)}\tilde{H}P^{(1,0)} + R^{(1,0)}\left\{\overline{\tilde{H}S}^{(1,0)}\right\}P^{(1,0)} = R^{(1,0)}\left\{\overline{S^{(1,0)}\tilde{H}_{\text{eff}}}\right\}P^{(1,0)}, \tag{13}$$

where the symbol 'tilde' means that the transformed Hamiltonian ($\tilde{H}$) is constructed using the CC amplitudes $\tilde{T}_1$ ($\equiv S_1^{(0,0)}$) and $\tilde{T}_2$ ($\equiv S_2^{(0,0)}$) only obtained at CCSDT1-A level of approximation for the ground-state calculation.

The projectors for the doublet model space $P^{(1,0)}$ and for the doublet virtual subspaces $Q^{(1,0)}$ and $R^{(1,0)}$ for N-electron system, respectively, are

$$P^{(1,0)} = \sum_{\alpha=1}^{M_P} |\phi_\alpha\,(N-1)\rangle\langle\phi_\alpha(N-1)|\,, \tag{14}$$

$$Q^{(1,0)} = \sum_{\alpha\beta p}^{N_D} \left|\phi^p_{\alpha\beta}\,(N-1)\rangle\langle\phi^p_{\alpha\beta}(N-1)\right|, \tag{15}$$

$$R^{(1,0)} = \sum_{\alpha\beta\gamma pq}^{N_T} \left|\phi^{pq}_{\alpha\beta\gamma}\,(N-1)\rangle\langle\phi^{pq}_{\alpha\beta\gamma}(N-1)\right|, \tag{16}$$

where $\alpha, \beta, \gamma, \ldots$. refer to occupied spin orbitals (holes) and $p, q, \ldots$, refer to unoccupied spin orbitals. M_P, N_D, N_T are the dimensions of the P-, Q- and R subspaces, respectively.

With

$$S^{(1,0)} = S_2^{(1,0)} + S_3^{(1,0)}, \tag{17}$$

where all unfrozen holes are active so that no $S_1^{(1,0)}$ appears in the calculation, the EIP-MRCCSDτ equations become

$$P^{(1,0)}\tilde{H}P^{(1,0)} + P^{(1,0)}\left\{\overline{\tilde{H}S_2^{(1,0)}}\right\}P^{(1,0)} + P^{(1,0)}\left\{\overline{\tilde{H}S_3^{(1,0)}}\right\}P^{(1,0)} = \tilde{H}^{(1,0)}_{\text{eff}} \tag{18}$$

$$Q^{(1,0)}\tilde{H}P^{(1,0)} + Q^{(1,0)}\left\{\overline{\tilde{H}S_2^{(1,0)}}\right\}P^{(1,0)} + Q^{(1,0)}\left\{\overline{\tilde{H}S_3^{(1,0)}}\right\}P^{(1,0)} = Q^{(1,0)}\left\{\overline{S_2^{(1,0)}\tilde{H}_{\text{eff}}}\right\}P^{(1,0)} \tag{19}$$

$$R^{(1,0)}\tilde{H}P^{(1,0)} + R^{(1,0)}\left\{\overline{\tilde{H}S_2^{(1,0)}}\right\}P^{(1,0)} + R^{(1,0)}\left\{\overline{\tilde{H}S_3^{(1,0)}}\right\}P^{(1,0)} = R^{(1,0)}\left\{\overline{S_3^{(1,0)}\tilde{H}_{\text{eff}}}\right\}P^{(1,0)} \tag{20}$$

as $QR = 0$ and $RQ = 0$ in the RHS of eq. (12) and eq. (13), respectively.

Projection of eqs (11)–(13) from the left on $\langle\phi_\alpha\,(N-1)\,|s$, $\langle\phi^p_{\alpha\beta}\,(N-1)\,|s$ and $\langle\phi^{pq}_{\alpha\beta\gamma}\,(N-1)\,|s$ respectively, and projection of all three equations on $|\phi_\alpha\,(N-1)\rangle s$ from the right, and writing $\sum_2^{(1,0)}$ and $\sum_3^{(1,0)}$ matrices in relation to the $S_2^{(1,0)}$ and $S_3^{(1,0)}$ amplitudes, lead to

$$Y_{PP} + Y_{PQ}\sum_2^{(1,0)} + Y_{PR}\sum_3^{(1,0)} = \tilde{H}^{(1,0)}_{\text{eff}} \tag{21}$$

$$Y_{QP} + Y_{QQ}\sum_2^{(1,0)} + Y_{QR}\sum_3^{(1,0)} = \sum_2^{(1,0)}\tilde{H}^{(1,0)}_{\text{eff}} \tag{22}$$

$$Y_{RP} + Y_{RQ}\sum_2^{(1,0)} + Y_{RR}\sum_3^{(1,0)} = \sum_3^{(1,0)}\tilde{H}^{(1,0)}_{\text{eff}}. \tag{23}$$

Introducing $\sum_2^{(1,0)} = X_{QP}X_{PP}^{-1}$ and $\sum_3^{(1,0)} = X_{RP}X_{PP}^{-1}$, and following refs [24,26], it leads to the EIP-MRCCSDτ equations in matrix form,

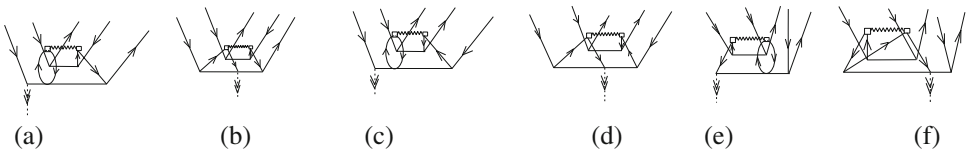

Figure 2. Goldstone diagrams relating to the three-body transformed Hamiltonian $\tilde{H}_3 = \{\overline{V\tilde{T}_2}\}_3$ contracted with connected triples for ionisation $S_3^{(1,0)}$.

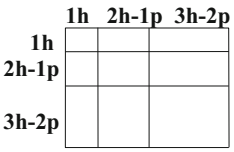

Figure 3. Various blocks of EIP-MRCCSDτ matrix for IP calculation.

$$\begin{bmatrix} Y_{PP} & Y_{PQ} & Y_{PR} \\ Y_{QP} & Y_{QQ} & Y_{QR} \\ Y_{RP} & Y_{RQ} & Y_{RR} \end{bmatrix}_{(N_{DT}+M_P)X(N_{DT}+M_P)} \times \begin{bmatrix} X_{PP} \\ X_{QP} \\ X_{RP} \end{bmatrix}_{(N_{DT}+M_P)XM_P} = \begin{bmatrix} X_{PP} \\ X_{QP} \\ X_{RP} \end{bmatrix}_{(N_{DT}+M_P)XM_P} \times \left[E_{PP}^{(1,0)}\right]_{M_PXM_P}, \quad (24)$$

where $N_{DT} = N_D + N_T$ and $[E_{PP}^{(1,0)}]$ consist of the IPs as direct difference energies.

In this article, we are concerned with the effect of three-body transformed Hamiltonian through full connected triples $\overline{\tilde{H}_3 S_3^{(1,0)}}$ (figure 2) in IP calculation by EIP-MRCCSDτ method. $\overline{\tilde{H}_3 S_3^{(1,0)}}$ appears in the $3h2p-3h2p$ block of EIP-MRCCSDτ matrix (figure 3) only. The dimension of EIP-MRCCSDτ matrix increases enormously compared to that of EIP-MRCCSD matrix because the inclusion of triples increases the N-electron functions manifold (for cc-pVTZ basis) so as to determine the eigenvalues by iterative Rettrup algorithm [37]. Only six Goldstone diagrams (figure 2) arise from the term $\overline{\tilde{H}_3 S_3^{(1,0)}}$. Large amount of computer operations is involved with these diagrams. Clearly, as $\tilde{H}_3$ is only $\{\overline{V\tilde{T}_2}\}_3$, the term may be supposed to contribute very little compared to the usual terms $\overline{\tilde{V}_3 S_3^{(1,0)}}$, where

$$\tilde{V} = V + \{\overline{V\tilde{T}_1}\}_2 + \frac{1}{2}\{\overline{V\tilde{T}_1\tilde{T}_1}\}_2 + \{\overline{V\tilde{T}_2}\}_2.$$

It is to be emphasised that figure 4 requires the maximum number of computer operations amongst all the diagrams representing $\overline{\tilde{V}_3 S_3^{(1,0)}}$. $\tilde{H}_3$ appears in

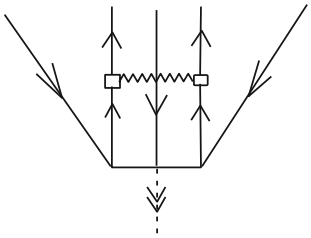

Figure 4. Goldstone diagram relating to a two-body transformed Hamiltonian $\tilde{V}$, contracted with triples for ionisation $S_3^{(1,0)}$.

$2h1p-2h1p$, $3h2p-1h$ and $3h2p-2h1p$ blocks also of the EIP-MRCCSDτ matrix but none having connected triples $S_3^{(1,0)}$ for ionised states. Some diagrams of $3h2p-2h1p$ block involve a large amount of computer operations while other such diagrams involve lower number of operations. All diagrams of these three blocks are always included in the calculation. A reasonable question may now arise. What if we suppress $\overline{\tilde{H}_3 S_3^{(1,0)}}$ from the computation assuming that their values are negligibly small? For illustration, moderately big molecules such as benzene, pyridine etc. when involve cc-pVQZ basis (or bigger ones), the speed of computation may be stymied severely if $\overline{\tilde{H}_3 S_3^{(1,0)}}$ is included. How much will the effect be on the accuracy of the results if it is excluded? This is the main aim of this work. For investigation, we have chosen two molecules Cl_2 and F_2. Since we calculated all valence IPs and plenty of satellite IPs up to ∼45 eV, we have taken relatively smaller basis sets, cc-pVDZ and cc-pVTZ, and did not take bigger basis as it would consume extraordinarily high time which our present computational facilities cannot tackle with. But more importantly, this exclusion seems to cause nothing serious because the above two basis sets illustrate the principal feature of the work quite well, that is, the difference of the theoretical IP profiles with and without the inclusion of $\overline{\tilde{H}_3 S_3^{(1,0)}}$.

3. Computational aspect

The effect of triples $S_3^{(0,0)} (= T_3)$ is estimated by using the CCSDT1-A model of Bartlett *et al* [30] for ground-

state coupled cluster calculation. In this model, $T_3 = \{\overline{VT}_2/\Delta\varepsilon\}_3$ (diag. 1 in figure 4 of ref. [30]) where V is the two-body part of the exact Hamiltonian H in normal ordered form and T_2 is the two-body closed shell CC operator, which by nature is in normal ordered form, and the curly-bracket { } represents normal ordering. In the starting iteration of CCSDT1-A calculation, the converged full CCSD T_2 amplitudes are used in the expression for T_3. T_3 is substituted in the T_1 determining equation (eq. (17) and diag. 6 in figure 2 of ref. [30]) and in the T_2 determining equation (eq. (18) and diag. 6 in figure 3 of ref. [30]), and then again the CCSD computer program is run till the convergence of the ground-state correlation energy at the CCSDT1-A level is achieved. The resulting one-body and two-body CC amplitudes are denoted by $\tilde{T}_1$ and $\tilde{T}_2$, respectively, which are stored and used to construct the transformed Hamiltonian

$$\tilde{H} = \overline{\{H(\exp(\tilde{T}_1 + \tilde{T}_2))\}}.$$

Thus, the open diagrams of $\tilde{H}$ contains one-body ($\tilde{f}$), two-body ($\tilde{V}$) and three-body ($\tilde{H}$) parts only in the EIP-MRCCSDτ calculation. (For the entire set of EIP-MRCCSDτ diagrams for IP calculation, see figures 1 and 2 of ref. [32]. For the determination of guess eigenvectors, see refs [23,31,32]). In order to observe the role of three-body transformed Hamiltonian through full connected triples $\overline{\tilde{H}_3 S_3^{(1,0)}}$ [25] in terms of magnitude, we performed two kinds of computations, scheme A and scheme B. Scheme A includes $\overline{\tilde{H}_3 S_3^{(1,0)}}$ along with the other usual diagrams for EIP-MRCCSDτ matrix [2,31,32,36], whereas in scheme B, this term is absent.

4. Results and discussion

In these calculations, two chemically interesting and challenging molecules Cl_2 and F_2 (fluorine atom is the most electronegative and Cl_2 contains as many as 34 electrons) are considered. The basis sets cc-pVDZ and cc-pVTZ (spherical Gaussians) and experimental equilibrium geometry are used in these computations. In our calculations the basis sets were collected from http://www.emsl.pnl.gov:2080/forms/basisform.html. Both molecules are linear and centrosymmetric and hence their point group is $D_{\infty h}$ out of which we consider only the largest Abelian subgroup D_{2h}. All outer valence main vertical IPs are presented in table 1. Since independent particle model is valid here, some Koopmans configurations appear while moving from one basis to another. Naturally, there are some one-to-one correspondences between scheme A and scheme B also. For the single bonded molecule F_2, the contribution of

Table 1. Contribution of the diagrams for three-body transformed Hamiltonian of $3h2p$–$3h2p$ block of EIP-MRCCSDτ matrix (figure 3) to vertical ionisation potentials (in eV) of outer valence region (relative intensities are in parentheses).

Molecule	States	Configurations	Basis: cc-pVDZ			Basis: cc-pVTZ			Expt.
			Scheme-A	Scheme-B	|Diff| (eV)	Scheme-A	Scheme-B	|Diff| (eV)	
F_2	$^2\Pi_g$	$1\pi_g^{-1}$	15.124 (0.933)	15.136 (0.932)	0.012	15.415 (0.928)	15.429 (0.927)	0.014	15.87[a]
									15.70[b]
	$^2\Pi_u$	$1\pi_u^{-1}$	18.190 (0.873)	18.216 (0.867)	0.026	18.492 (0.874)	18.521 (0.869)	0.029	18.8[a]
									18.4[b]
Cl_2	$^2\Sigma_g^+$	$3\sigma_g^{-1}$	20.671 (0.956)	20.652 (0.954)	0.019	20.926 (0.948)	20.908 (0.947)	0.018	21.1[a]
	$^2\Pi_g$	$2\pi_g^{-1}$	11.138 (0.954)	11.136 (0.954)	0.002	11.318 (0.948)	11.315 (0.948)	0.003	11.49[b]
	$^2\Pi_u$	$2\pi_u^{-1}$	14.037 (0.059)	13.997 (0.916)	0.040	14.162 (0.911)	14.160 (0.911)	0.002	14.0[b]
	$^2\Sigma_g^+$	$5\sigma_g^{-1}$	15.687 (0.952)	17.446 (0.018)	0.021	15.806 (0.942)	15.792 (0.942)	0.014	15.8[b]
			17.467 (0.018)				19.698 (0.008)		

[a]Ref. [38].
[b]Ref. [39].

Table 2. Contribution of the diagrams for three-body transformed Hamiltonian of $3h2p-3h2p$ block of EIP-MRCCSDτ matrix (figure 3) to inner valence main and satellite vertical ionisation potentials (in eV) of F_2 and Cl_2.

Mol	States	Basis: cc-pVDZ			Basis: cc-pVTZ			Expt.
		Scheme A	Scheme B	|Diff| (eV)	Scheme A	Scheme B	|Diff| (eV)	
F_2	$^2\Sigma_g^+$	29.680(0.016)	28.863(0.015)	0.817		41.961(0.617)		
		40.785(0.043)	40.835(0.015)	0.05	41.916(0.659)	42.910(0.149)	0.045	41.75[a]
		42.672(0.436)	42.653(0.047)	0.019	42.800(0.157)	42.385(0.059)	0.11	
		50.701(0.056)	50.600(0.060)	0.101	42.889(0.048)	50.367(0.032)	0.504	
		54.836(0.101)	53.719(0.056)	1.117	50.482(0.190)		0.115	
	$^2\Pi_u$	24.524(0.028)	24.461(0.032)	0.063	25.014(0.026)	24.940(0.029)	0.074	
		32.416(0.065)	31.643(0.050)	0.773	32.936(0.039)	32.025(0.052)	0.911	
		33.151(0.014)						
		33.671(0.021)						
		45.999(0.011)						
			44.431(0.020)					
			50.239(0.020)					
	$^2\Pi_g$	41.063(0.021)	40.314(0.067)	0.749		40.691(0.047)		
		42.117(0.013)			42.491(0.011)			
		47.846(0.022)			48.659(0.013)			
	$^2\Sigma_u^+$	29.110(0.015)	28.857(0.012)	0.253	29.690(0.030)			
		29.203(0.040)			29.762(0.038)	29.432(0.039)	0.33	
		32.669(0.017)	32.413(0.017)	0.256	33.195(0.022)	32.928(0.023)	0.267	
		37.491(0.675)	37.480(0.743)	0.011		37.289(0.667)		37.47[a]
Cl_2	$^2\Sigma_g^+$	22.222(0.027)	22.137(0.026)	0.085	22.443(0.034)	22.356(0.033)	0.087	
		25.085(0.013)	25.041(0.012)	0.044	26.423(0.019)	26.637(0.019)	0.214	
		28.214(0.650)	28.202(0.635)	0.012	26.655(0.073)	26.684(0.059)	0.029	
		29.962(0.020)	29.739(0.029)	0.223	27.479(0.164)	27.477(0.152)	0.002	
		37.302(0.038)	37.237(0.038)	0.065	29.939(0.032)	31.244(0.048)	1.305	
					34.358(0.021)			
						35.631(0.048)		
	$^2\Pi_u$		23.119(0.083)					
					22.974(0.059)	22.967(0.059)	0.007	
						27.466(0.002)		
						29.075(0.002)		
						29.514(0.003)		
						30.663(0.002)		
					31.017(0.017)	31.000(0.018)	0.017	
						31.258(0.009)		
	$^2\Pi_g$				22.607(0.002)			
		25.579(0.029)	25.412(0.023)	0.167	25.606(0.015)	25.534(0.011)	0.072	
						26.019(0.006)		
					31.139(0.002)	31.076(0.002)	0.063	
					33.351(0.014)	33.308(0.008)	0.043	
					33.470(0.012)	33.404(0.011)	0.066	
						34.099(0.003)		
						34.804(0.003)		
					34.804(0.010)	34.844(0.011)	0.04	
						36.413(0.007)		
						37.059(0.002)		
						37.728(0.002)		
						38.080(0.002)		
						38.619(0.001)		
						48.067(0.001)		
		22.258(0.297)	22.222(0.275)	0.036	22.404(0.424)	22.376(0.341)	0.028	

Table 2. *Continued.*

Mol	States	Basis: cc-pVDZ			Basis: cc-pVTZ			Expt.
		Scheme A	Scheme B	|Diff| (eV)	Scheme A	Scheme B	|Diff| (eV)	
	$^2\Sigma_u^+$	24.399(0.279)	24.339(0.289)	0.06	24.413(0.111)	24.413(0.274)	0	
		26.268(0.185)	26.220(0.184)	0.048	26.214(0.071)			
		38.132(0.025)	38.082(0.023)	0.05	31.646(0.033)	31.587(0.032)	0.059	
					34.124(0.021)	34.076(0.022)	0.048	
						34.454(0.029)		
					36.911(0.042)	36.803(0.045)	0.108	
					37.325(0.013)	38.207(0.027)	0.882	
		41.469(0.025)	40.200(0.018)	1.269				

[a]Ref. [40]

$\overline{\tilde{H}_3 S_3^{(1,0)}}$ is small. For $^2\Pi_u$ state, the differences in the case of cc-pVDZ and cc-pVTZ are 0.026 eV and 0.029 eV respectively. For $^2\Pi_u$ state of Cl_2, the difference (cc-pVDZ) 0.040 eV is significant. In view of that we are considering here the correlation dynamics of outer valence electrons.

Experimental IPs are presented in the tables with a view to realise the reliability of our theoretical results only. Too accurate comparison is not possible here because of the restraint of our starting basis sets. For that, approaching towards basis set saturation as much as possible is necessary. Since scheme A (as it includes $\overline{\tilde{H}_3 S_3^{(1,0)}}$) gives more accurate IP, from now on or unless otherwise explicitly mentioned, it will be assumed that a theoretical IP value relates to scheme A only.

In the inner valence region, the sizes of the basis sets sometimes influence the IP-profile of the same molecule in higher energy regions considerably. The single-bonded F_2 molecule is studied first, the IPs of which are presented in table 2. The calculation of F_2 was performed at experimental internuclear distance 1.4199 a.u. Ground configuration of F_2 is $^1\Sigma_g^1 : 1\sigma_g^2 1\sigma_u^2 2\sigma_g^2 2\sigma_u^2 1\pi_u^2\, 1\pi_u'^2 3\sigma_g^2 1\pi_g^2 1\pi_g'^2$). Two virtual orbitals were kept frozen for cc-pVDZ and cc-pVTZ basis in post Hartree–Fock calculations. The EIP-VUMRCCSDτ bar spectra are given in figure 5. Our results of outer valence region (table 1) at truncation threshold 25.0 a.u. are within 0.3 eV of experiments (see refs [39,40]) for cc-pVTZ basis. After 20 eV (see table 2), the formidable intruder state problem becomes active for which nonlinear VUMRCC method for (1-hole, 0-particle sector) does not work and one then has to apply EIP-VUMRCC method. The first $^2\Sigma_g^+$ satellite of F_2 shows that maximum contribution of $\overline{\tilde{H}_3 S_3^{(1,0)}}$ is 1.117 eV for cc-pVDZ basis and 0.504 eV for cc-pVTZ basis. The difference (cc-pVTZ) 1.117 eV for $^2\Sigma_g^+$ is significant. In $^2\Pi_u$ state, the maximum contributions are 0.773 eV for cc-pVDZ basis and 0.911 eV for cc-pVTZ basis respectively. In $^2\Sigma_u^+$ state, the contributions are 0.256 eV for cc-pVDZ basis and 0.267 eV for cc-pVTZ basis. Other satellites do not have the basis-to-basis correspondence. However, scheme A to scheme B correspondence is retained, which is based on the dominant configurations with expansion coefficient ∼0.3 or more.

The next test case is Cl_2 molecule, the IPs of which are presented in table 2. The calculation of Cl_2 was performed at an experimental internuclear distance 1.99 a.u. Ground configuration of Cl_2 is $^1\Sigma_g^1 : 1\sigma_g^2 1\sigma_u^2 2\sigma_g^2 2\sigma_u^2 3\sigma_g^2 3\sigma_u^2 1\pi_u^2\, 1\pi_u'^2 1\pi_g^2 1\pi_g'^2 4\sigma_g^2 4\sigma_u^2 5\sigma_g^2 2\pi_u'^2 2\pi_u^2 2\pi_g'^2 2\pi_g^{2)}$. Two virtual orbitals were kept frozen for cc-pVDZ and cc-pVTZ basis in post Hartree–Fock calculations. The EIP-VUMRCCSDτ bar spectra are given in figure 6. Our result of the outer valence region (table 1) at truncation threshold 25.0 a.u. are within 0.3 eV of experiments (see refs [39,40]) for cc-pVTZ basis. The first $^2\Sigma_g^+$ satellite of Cl_2 shows that maximum contribution of $\overline{\tilde{H}_3 S_3^{(1,0)}}$ is by an amount 0.223 eV for cc-pVDZ basis and 1.305 eV for cc-pVTZ basis, respectively. In $^2\Pi_u$ state, the contribution is 0.167 eV for cc-pVDZ basis. In $^2\Sigma_u^+$ state, the maximum contribution is 1.269 eV for cc-pVDZ basis, no such value for cc-pVTZ basis is found.

The IPs onwards are arranged on the basis of dominant configurations. If dominant configurations differ from basis-to-basis substantially, they are put in different rows in the tables. Thus, some IP values which appear for cc-pVDZ may not appear at all for cc-pVTZ, and vice versa. Similarly, an IP for a basis appearing in scheme A may be absent in scheme B, and vice versa. While in the first case it is due to basis-set effect, in the second case it is due to $\overline{\tilde{H}_3 S_3^{(1,0)}}$. If for an IP, scheme A to scheme B correspondence is observed, only then it is possible to make a comment on the amount by which the IP has been shifted to what extent in scheme B relative to scheme A. In other words, a quantitative picture of

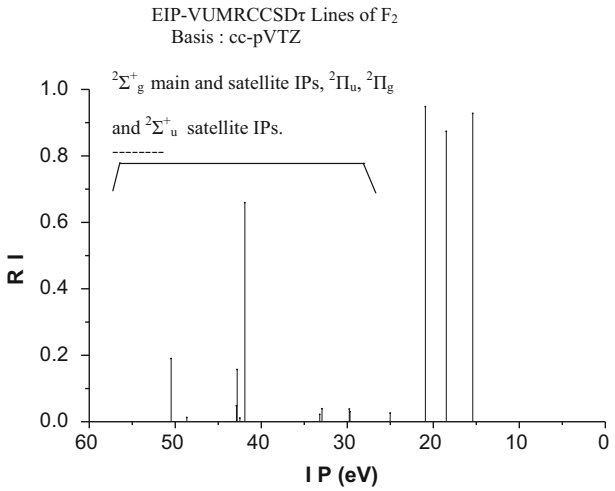

Figure 5. Vertical valence main and satellite IPs computed at a truncation energy threshold of 25 a.u. of F_2.

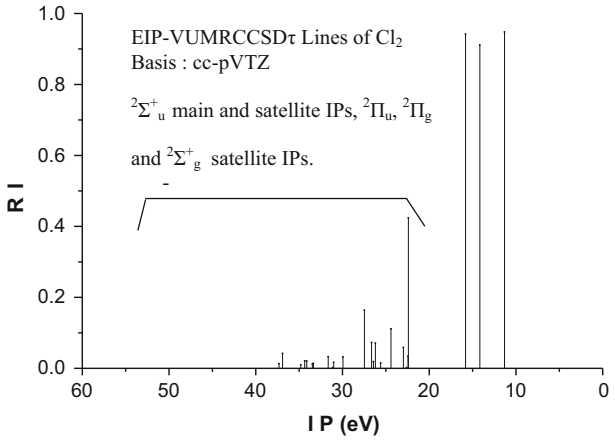

Figure 6. Vertical valence main and satellite IPs computed at a truncation energy threshold of 25 a.u. of Cl_2.

the effect of $\overline{\tilde{H}_3 S_3^{(1,0)}}$ can be made. For quite a few IPs, the contributions of $\overline{\tilde{H}_3 S_3^{(1,0)}}$ are significant. The values mentioned in parenthesis are relative intensities along with IPs.

In the inner valence region, due to the breakdown of independent particle model, each energy level is split into multiple energy states. In the inner valence region, the sizes of the basis sets sometimes influence the IP profile of the same molecule in higher energy regions considerably.

In our calculations, we have used cc-pVDZ and cc-pVTZ bases. As we use larger and larger bases, the calculated value of ionisation potential approaches experimental observations. In order to make a comparison with the experimental observations, one should use (relatively) large, say, aug-cc-pVQZ basis.

5. Conclusion

EIP-MRCC method is employed for investigating the effect of three-body transformed Hamiltonian $\left(\tilde{H}_3\right)$ through full connected triples $S_3^{(1,0)}$ on the main and satellite ionisation potentials (IPs) of molecular systems such as Cl_2 and F_2. $\tilde{H}_3$ is constructed based on high performing CCSDT1-A model for triples in ground-state energy calculation. The Goldstone diagrams for $\overline{\tilde{H}_3 S_3^{(1,0)}}$ appear only in the enormously large $3h2p-3h2p$ block of the EIP-MRCCSDτ matrix for IP calculation. Some related diagrams involve large amount of computer operations which may require high computation time for evaluation of IPs. In view of that, one may hesitate to include these diagrams when working with moderately big molecules such as benzene, pyridine etc. In order to substantiate the theoretical evidences, we took two starting bases cc-pVDZ and cc-pVTZ. The present calculations show that for F_2 and Cl_2, the above-said effect sometimes is considerably high and may even be more than 0.910 eV (F_2: cc-pVTZ) and 1.257 eV (Cl_2: cc-pVDZ) which are much presumably due to the high electronegativity of F and Cl atoms. This suggests that inclusion of $\overline{\tilde{H}_3 S_3^{(1,0)}}$ is essential for high accuracy in EIP-VUMRCC IP calculations.

Acknowledgements

The fund for the work was provided by University Grants Commission, North Eastern Regional Office (MRP No. 5-379/2014-15/MRP/NERO/2231, dated 17 February 2015, FD Dairy No. 3206).

References

[1] C E Smith, R A King, T D Crawford, *J. Chem. Phys.* **122**, 054110 (2005)
[2] P H P Harbach, M Wormit and A Dreuw, *J. Chem. Phys.* **141**, 064113 (2014)
[3] A Dreuw and M Wormit, *WIREs Comput. Mol. Sci.* **5**, 82 (2015)
[4] S Chattopadhyay, R K Chaudhuri and U Sinha, *J. Comput. Chem*. **36**, 907 (2015)
[5] W Kutzelnigg, *Int. J. Quantum Chem.* **109**, 3858 (2009)
[6] M Saitow, Y Kurashige and T Yanai, *J. Chem. Theory Comput.* **11**, 5120 (2015)
[7] Y R Miao, C G Ning and J K Deng, *Phys. Rev. A* **83**, 062706 (2011)
[8] M Ehara, S Yasuda and H Nakatsuji, *Z. Phys. Chem.* **217**, 161 (2003)
[9] M Ehara, M Ishida and H Nakatsuji, *J. Chem. Phys.* **117**, 3248 (2002)

[10] M Musial, A Perera and R J Bartlett, *J. Chem. Phys.* **134**, 114108 (2011)
[11] J R Gour and P Piecuch, *J. Chem. Phys.* **125**, 234107 (2006)
[12] J Shen and P Piecuch, *Mol. Phys.* **112**, 868 (2014)
[13] K Kowalski and P Piecuch, *J. Chem. Phys*. **115**, 643 (2001)
[14] S Chattopadhyay, U Sinha Mahapatra and R K Chaudhuri, *Mol. Phys.* **112**, 2720 (2014)
[15] M K Nayak, R K Chaudhuri, S Chattopadhyay and U S Mahapatra, *J. Mol. Struct.: Theochem.* **768**, 133 (2006)
[16] D Jana, D Datta and D Mukherjee, *Chem. Phys*. **329**, 290 (2006)
[17] D Mukherjee, *Chem. Phys. Lett.* **125,** 207 (1986)
[18] R J Bartlett and M Musial, *Rev. Mod. Phys*, **79**, 291 (2007)
[19] F A Evangelista, A C Simmonett, W D Allen, H F Schaefer III and J Gauss, *J. Chem. Phys.* **128**, 124104 (2008)
[20] I Shavitt and R J Bartlett, *Many-body methods in chemistry and physics: Many-body perturbation theory and coupled-cluster methods* (Cambridge Press, New York, 2009)
[21] P Cársky, J Paldus and J Pittner, *Recent progress in coupled cluster methods: Theory and applications* (Springer Science and Business Media, 2010)
[22] J Singh, K L Baluja and G Longiany, *Pramana – J. Phys.* **88**, 76 (2017)
[23] D Sinha, S K Mukhopadhyay, R Chaudhuri and D Mukherjee, *Chem. Phys. Lett.* **154**, 544 (1989)
[24] D Mukhopadhyay, S Mukhopadhyay, R Chaudhuri and D Mukherjee, *Theor. Chim. Acta* **80**, 441 (1991)
[25] K Adhikari, S Chattopadhyay, R K Nath, B K De and D Sinha, *Chem. Phys. Lett.* **474**, 199 (2009)
[26] S Chattopadhyay and D Mukhopadhyay, *J. Phys. B* **40**, 10 (2007)
[27] U Sinha Mahapatra and S Chattopadhyay, *J. Chem. Phys*. **133**, 074102 (2010)
[28] R Chaudhuri, D Mukhopadhyay and D Mukherjee, *Chem. Phys. Lett.* **162**, 393 (1989)
[29] A Mitra, U S Mahapatra, D Majumder and D Sinha, *J. Phys. Chem. A* **102**, 7277 (1998)
[30] Y S Lee, S A Kucharski and R J Bartlett, *J. Chem. Phys.* **81**, 5906 (1984)
[31] S Chattopadhyay, A Mitra, D Jana, P Ghosh and D Sinha, *Chem. Phys. Lett.* **361**, 298 (2002)
[32] S Chattopadhyay, A Mitra and D Sinha, *J. Chem. Phys.* **125**, 244111 (2006)
[33] K Adhikari, S Chattopadhyaya, B K De, A Sharma, P K Nath and D Sinha, *J. Comput.Chem.* **34**, 1291 (2013)
[34] S Kabakçi, B Karaçoban Usta and L Özdemir, *Pramana – J. Phys*. **85**, 691 (2015)
[35] J A R Coope and D W Sabo, *J. Comput. Phys.* **23**, 404 (1977)
[36] A Sharma, S Chattopadhyay, K Adhikari and D Sinha, *Chem. Phys. Lett.* **634**, 88 (2015)
[37] S Rettrup, *J. Comput. Phys.* **45**, 100 (1982)
[38] G Bieri, A Schemelzer, L Åsbrink and M Jonsson, *Chem. Phys.* **49**, 213 (1980)
[39] A B Cornfored, D C Frost, C A McDowell, J L Ragle and I A Stenhouse, *J. Chem. Phys.* **54**, 2651 (1971)
[40] P Weightman, T D Thomas and D R Jennison, *J. Chem. Phys.* **78**, 1652 (1983)